

---

# Princeton Plasma Physics Laboratory

---

PPPL-

PPPL-



Prepared for the U.S. Department of Energy under Contract DE-AC02-09CH11466.

# Princeton Plasma Physics Laboratory

## Report Disclaimers

---

### Full Legal Disclaimer

This report was prepared as an account of work sponsored by an agency of the United States Government. Neither the United States Government nor any agency thereof, nor any of their employees, nor any of their contractors, subcontractors or their employees, makes any warranty, express or implied, or assumes any legal liability or responsibility for the accuracy, completeness, or any third party's use or the results of such use of any information, apparatus, product, or process disclosed, or represents that its use would not infringe privately owned rights. Reference herein to any specific commercial product, process, or service by trade name, trademark, manufacturer, or otherwise, does not necessarily constitute or imply its endorsement, recommendation, or favoring by the United States Government or any agency thereof or its contractors or subcontractors. The views and opinions of authors expressed herein do not necessarily state or reflect those of the United States Government or any agency thereof.

### Trademark Disclaimer

Reference herein to any specific commercial product, process, or service by trade name, trademark, manufacturer, or otherwise, does not necessarily constitute or imply its endorsement, recommendation, or favoring by the United States Government or any agency thereof or its contractors or subcontractors.

---

## PPPL Report Availability

### Princeton Plasma Physics Laboratory:

<http://www.pppl.gov/techreports.cfm>

### Office of Scientific and Technical Information (OSTI):

<http://www.osti.gov/bridge>

---

### Related Links:

[U.S. Department of Energy](#)

[Office of Scientific and Technical Information](#)

[Fusion Links](#)

## Response of NSTX liquid lithium divertor to high heat loads

T. Abrams<sup>a,\*</sup>, M.A. Jaworski<sup>a</sup>, J. Kallman<sup>b</sup>, R. Kaita<sup>a</sup>, E.L. Foley<sup>c</sup>, T.K. Gray<sup>d</sup>, H. Kugel<sup>a</sup>,  
F. Levinton<sup>c</sup>, A.G. McLean<sup>b</sup>, and C.H. Skinner<sup>a</sup>

<sup>a</sup>*Princeton Plasma Physics Laboratory, Princeton, NJ, 08543, USA.*

<sup>b</sup>*Lawrence Livermore National Laboratory, Livermore, CA, 94550, USA.*

<sup>c</sup>*Nova Photonics, Inc., Princeton, NJ, 08543, USA.*

<sup>d</sup>*Oak Ridge National Laboratory, Oak Ridge, TN, 37831, USA.*

### Abstract

Samples of the NSTX Liquid Lithium Divertor (LLD) with and without an evaporative Li coating were directly exposed to a neutral beam *ex-situ* at a power of  $\sim 1.5$  MW/m<sup>2</sup> for 1-3 seconds. Measurements of front face and bulk sample temperature were obtained. Predictions of temperature evolution were derived from a 1D heat flux model. No macroscopic damage occurred when the “bare” sample was exposed to the beam but microscopic changes to the surface were observed. The Li-coated sample developed a lithium hydroxide (LiOH) coating, which did not change even when the front face temperature exceeded the pure Li melting point. These results are consistent with the lack of damage to the LLD surface and imply that heating alone may not expose pure liquid Li if the melting point of surface impurities is not exceeded. This suggests that flow and heat are needed for future PFCs requiring a liquid Li surface.

---

*PACS:* 52.70.Kz, 52.40.Hf, 44.30.+v

*PSI-20 Keywords:* Divertor material, Lithium coating, Infrared thermography

*\*Corresponding author address:* PPPL, P.O. Box 451, Princeton, NJ 08543-0451

*\*Corresponding author e-mail:* tabrams@pppl.gov

*Presenting author:* Tyler Abrams

*Presenting author e-mail:* tabrams@pppl.gov

## 1. Introduction

One of the most prominent issues barring the path to magnetically confined fusion reactors involves developing plasma-facing components (PFCs) that can withstand the high heat and particle fluxes in a reactor environment. Recent experiments with Li-coated PFCs on the National Spherical Torus eXperiment (NSTX) have shown evidence of improved confinement and ELM reduction[1]. The LLD was installed on NSTX in 2010 to test the concept of a Li-coated porous Mo surface. While the LLD was intended to provide a Li PFC, there was a concern that the liquid Li could be ejected and expose the Mo substrate[2]. It was thus useful to test the Mo surface as a low-sputtering PFC and the ability of a thin surface layer to allow heat transmission to an underlying copper heat sink.

*In-situ* head load testing of the LLD is difficult due to the complex tokamak environment in which it resides. This motivated offline heat load testing where heat and particle sources can be carefully controlled and studied. The primary goal of these experiments was to determine if the “bare” LLD surface would experience significant physical damage during NSTX divertor heat loading. The secondary motivation was to quantify any microscopic damage that may result on the porous Mo surface due to plasma bombardment.

Initial experiments were performed using the hydrogen diagnostic neutral beam (DNB) for the Motional Stark Effect Laser Induced Fluorescence (MSE-LIF) diagnostic system[3,4] on NSTX. The DNB was used to simulate the high heat and particle fluxes in the NSTX divertor. A small prototype LLD sample was repeatedly bombarded by the DNB at a peak heat flux of  $\sim 1.5 \text{ MW/m}^2$ . Subsequent heat loading experiments were performed using a second prototype sample that was coated with a  $150 \text{ }\mu\text{m}$  Li layer. The primary goal of this experiment was to quantify the effects of high heat flux on a Li-coated Mo substrate. A secondary goal was to examine the extent and effects of Li passivation on the LLD surface.

The temporal and spatial evolution of the surface temperature was monitored using an infrared (IR) camera as well as two embedded thermocouples. A thermal analysis of the IR data was subsequently performed using 1D analytic model to calculate heat fluxes. These calculations were corroborated with calorimetry measurements obtained from thermocouple data. Optical microscopy was performed on both samples at 10x magnification before and after exposure to the DNB, and for the Li-coated sample, before and after cleaning. The resulting images were analyzed with an image-processing algorithm. The primary result presented in this paper is the output of this algorithm: spatially-resolved “damage” profiles which quantify microscopic changes in sample surface morphology due to bombardment by the DNB.

## **2. Materials and Methods**

The LLD and the prototype samples consist of a 152  $\mu\text{m}$  porous molybdenum (Mo) coating plasma-sprayed onto a 254  $\mu\text{m}$  of stainless steel, which is in turn explosively bonded to a 1.9 cm copper plate[5]. Each prototype LLD sample measures approximately 3.6 cm by 4.9 cm, yielding a surface area of about 18  $\text{cm}^2$ . Two type Type K thermocouples were cemented into small wells on the sample: one 2 mm behind the front face and another centered on the rear face.

Two strip heaters were affixed to the bottom face of the Li-coated sample using carbon cement. Approximately 140 mg of 99.9% pure solid Li was placed on the porous Mo surface inside an argon glove box. The temperature of the sample was raised above the 180  $^{\circ}\text{C}$  Li melting point and the Li was allowed to “wick” into the mesh with additional smoothing using a small “scraping” tool. The sample was placed in a sealed argon bag and transported to the DNB test chamber in an adjoining room. Despite efforts to minimize exposure time to full or partial atmosphere, it is believed that the Li layer had developed a lithium hydroxide (LiOH) coating in the period of time between Li application and DNB exposure.

### 3. Experimental Configuration

A diagram of the experimental setup is shown in Figure 1. The MSE-LIF DNB typically operates a hydrogen beam continuously at 30 kV with 28 mA of plasma current. The prototype sample was mounted on a linear-motion feed-through inside a six-way across approximately 1.5 m from the plasma source. The sample was angled at  $45^\circ$  with respect to the beam line to allow IR measurements to be captured by a camera outside the chamber. The camera provided 1 mm spatial resolution at a sampling rate of 30 Hz.

Initial exposures were performed on the “bare” LLD prototype sample. Subsequent exposures were performed on a Li-coated sample. The sample began in the retracted position. The sample was “plunged” down in the path of the neutral beam then quickly retracted after a specified time interval. Roughly 10 exposures were performed that varied in duration from 1 to 3 seconds. These durations were chosen in order to simulate a series of NSTX discharges that have a typical pulse length of 1 s. During each exposure, temperature measurements were recorded by an IR camera. A false-color image of the sample captured by the IR camera during beam operation is shown in Figure 2. Absolute temperatures were determined via an *ex-situ* calibration on the bare Mo sample and an additional *in-situ* calibration for the Li-coated sample. Front face and bulk sample temperatures were also recorded using the two embedded thermocouples.

## 4. Results and Discussion

### 4.1 Thermal Analysis of Heat Flux

The vertical temperature profile on the sample measured by the IR camera is shown in Figure 3. Both the horizontal and vertical profiles are assumed to be symmetric along axes extending through the center of the beam line, but are not completely radially symmetric due to

the 45° incidence angle of the neutral beam. These profiles are further assumed to follow a Maxwellian distribution and have a calculated half-width at half maximum (HWHM) of 0.9 cm and  $0.9 \cdot \cos(45^\circ) \approx 1.4$  cm, respectively. These parameters, in conjunction with calorimetry calculations using thermocouple data, are sufficient to calculate the net heat flux of the DNB as a function of position on the sample surface. A plot of bulk sample temperature rise against total exposure time is shown in Figure 4. A linear fit produces an average rate of net energy deposition to the sample  $\langle J \rangle \approx 1.0$  kJ/s. The net heat flux of the beam is thus modeled by:

$$q(x, y) = \frac{\langle J \rangle}{2\pi\sigma_x\sigma_y} \exp\left[\frac{-x^2}{2\sigma_x^2} + \frac{-y^2}{2\sigma_y^2}\right] \quad (1)$$

where x and y refer to the horizontal and vertical distance from the center of the beam along the surface of the sample. This calculation yields a peak heat flux  $q(0,0)$  of 1.2 MW/m<sup>2</sup>.

These calculated heat fluxes were benchmarked against a 1D analytic model which treats the copper bulk as a semi-infinite slab. The porous Mo, stainless steel, and Li layers were treated in the opposite (infinitely thin) limit, which approximates the temperature drop across each layer as  $\Delta z/k$ , where  $\Delta z$  is the layer thickness and k is thermal conductivity. Using the standard 1D treatment of thermal diffusion[6] and assuming constant heat flux q, one can model the thermal evolution of the sample by:

$$T(t, z = 0) = T_0 + q \left[ \left( \frac{4\alpha_{Cu}t}{\pi k_{Cu}^2} \right)^{1/2} + \frac{\Delta z_{Mo}}{k_{Mo}} + \frac{\Delta z_{SS}}{k_{SS}} + \frac{\Delta z_{Li}}{k_{Li}} \right] \quad (2)$$

where  $\alpha_{Cu}$  is the thermal diffusion coefficient for copper and  $T_0$  is the initial sample temperature in Kelvin. The  $\Delta z_{Li}/k_{Li}$  term was omitted during the bare sample analysis.

The thermal evolution of the sample surface at the center of the beam as a function of time for a bare sample exposure is shown in Figure 4. In order to obtain a satisfactory fit to this data with Equation 2, it was necessary to introduce a vertical offset as a free parameter. The

physical interpretation of this offset is poor thermal contact between the Mo and stainless steel layers within the LLD sample. This effect was modeled by allowing  $k_{Mo}$  to vary as a free parameter, introducing an “effective” thermal conductivity. This calculation yields a peak heat flux on the sample of  $1.5 \text{ MW/m}^2$  and an effective thermal conductivity  $k_{eff} = k_{Mo}/20$ .

The heat flux can also be calculated without assuming it is constant in time through numerical methods. A forward in time, centered in space (FTCS) finite-difference scheme[7] was applied to the thermal diffusion equation using the same boundary conditions as the analytic model.  $T_1^n$  and  $T_j^0$  are known for all  $n$  (time coordinate) and  $j$  (spatial coordinate), respectively, on the computational grid. Thus we obtain a well-posed problem with  $n$  equations and  $n$  unknowns that can be solved for  $q^n$  in terms of known values of  $T_j^n$ :

$$q^n = \frac{k_{Cu}}{\Delta x} \left\{ \left[ \frac{T_1^{n+1} - T_1^n}{\Delta t} \right] \frac{(\Delta z)^2}{\alpha_{Cu}} - T_2^n + T_1^n \right\} \quad (3)$$

The time-dependent heat fluxes at the center of the beam obtained with this numerical model are shown in Figure 5.

#### 4.2 Microscopic Analysis of Sample Morphology

Optical microscopy was performed on both samples using National Instruments Microscope DC3-4201, capable of up to 100x magnification. The images analyzed were captured at 10x magnification, which corresponds to a resolution of approximately  $1 \mu\text{m}/\text{pixel}$ . A “panorama” of images was produced by moving the sample in 1-2 mm increments across the Mo surface horizontally through the center of the beam exposure location. This procedure was performed before and after exposure to the DNB for the bare sample and after exposure for the Li-coated sample. Analysis of these images “by eye” before and after particle bombardment indicated no obvious microscopic damage to the “bare” or lithiated porous Mo surface.



These images were analyzed with ImageJ[8] to quantify possible microscopic changes in sample surface morphology. First, each full-color image was converted to 8-bit grayscale. Next, the images were converted to black and white using a user-defined “black threshold.” Pixels with intensities above this threshold were converted to black while the remaining pixels were converted to white. The two black thresholds used were 111 and 131. The resulting number of black regions on each image was tabulated and divided by the total black area to yield an average “particle size.” This average particle size measurement represents a quantitative characterization of the surface morphology captured in each image.

Average particle sizes as a function of position before and after beam exposure are plotted in Figure 6. The porous Mo layer is nearly uniform in average particle size prior to exposure. A smoothly varying pattern in the surface morphology is evident after beam exposure on the bare LLD sample that correlates with the Gaussian heat flux profile of the beam. The absence of significant macroscopic damage, however, is consistent with effective heat transmission through the thin surface layer to the underlying copper heat sink.

No such smoothly varying morphology pattern, however, is evident on the Li-coated LLD sample surface. This suggests that the surface did not melt during beam exposure tests in excess of 250 °C, which is well above the Li melting point 180 °C. As noted in Section 2, an impurity layer composed of LiOH formed on the lithiated surface. LiOH has a melting point of 462 °C, which was not reached during these experiments.

IR thermography analysis performed in [9] indicates that the plasma-facing surface of the LLD never exceeded 450 °C and typically operated in a temperature range from 200-300 °C. In addition, recent laboratory experiments[10] have shown that even at the  $10^{-8}$  torr partial pressures of water typically found in tokamaks, a LiOH impurity layer forms on a pure liquid lithium

surface within 150-200 seconds. This implies that during LLD operation in NSTX, a pure liquid lithium surface may not have been exposed to the plasma.

## **5. Conclusions**

Offline experiments at heat fluxes comparable to the NSTX divertor indicate that a layer comprised of Li compounds on the LLD surface will not melt or suffer significant erosion at temperatures in excess of 250 °C. Measurements have shown that a LiOH layer undergoes microscopic changes at this temperature but remains essentially intact. These results also underscore the difficulty of maintaining a pure Li surface under typical tokamak vacuum conditions. This effort is part of an ongoing investigation into the physical and chemical mechanisms behind this passivation process, the goal of which is to form a causal link between tokamak wall conditions and edge plasma behavior.

## **Acknowledgements**

This work is supported by US DOE contracts DE-AC02-09CH11466 and DE-AC05-00OR22725. Special appreciation is extended to the late John Timberlake for his invaluable assistance in lithium handling.

## **References**

- [1] H.W. Kugel *et al.*, Journal of Nuclear Materials 415 (2011) S400-S404.
- [2] D.G. Whyte *et al.*, Fusion Engineering and Design 72 (2004) 133-147.
- [3] E.L. Foley *et al.*, Rev. Sci. Instrum. 77, 10F311 (2006)
- [4] E.L. Foley, Ph. D. thesis, Princeton University (2005)
- [5] H.W. Kugel *et al.*, Fusion Engineering and Design (2011)
- [6] A.F. Mills, Heat and Mass Transfer, CRC Press, 1995.

- [7] W.H. Press *et al.*, Numerical Recipes: The Art of Scientific Computing, third ed., Cambridge University Press, New York, 2007.
- [8] M.D. Abramoff *et al.*, Biophotonics International 11 (7) (2004) 36-42.
- [9] A.G. McLean *et al.*, Journal of Nuclear Materials Submitted
- [10] C.H. Skinner *et al.*, Journal of Nuclear Materials Submitted

## List of Figures

1	A view of the experimental apparatus through the IR window mounted on one side of the six-way cross and the linear motion feed-thorough mounted on top of the cross.....	12
2	A false color image of the “bare” LLD sample during neutral beam exposure.....	13
3	Vertical temperature profile on the front face of the LLD sample .....	14
4	Thermal evolution of the front face of the bare LLD sample at the center of the beam during a ~1.8 s exposure.....	15
5	Heat flux at the center of the beam as determined from a 1-D numerical model ....	16
6	Average particle size plotted against distance across the surface of the bare sample and Li-coated sample.....	17

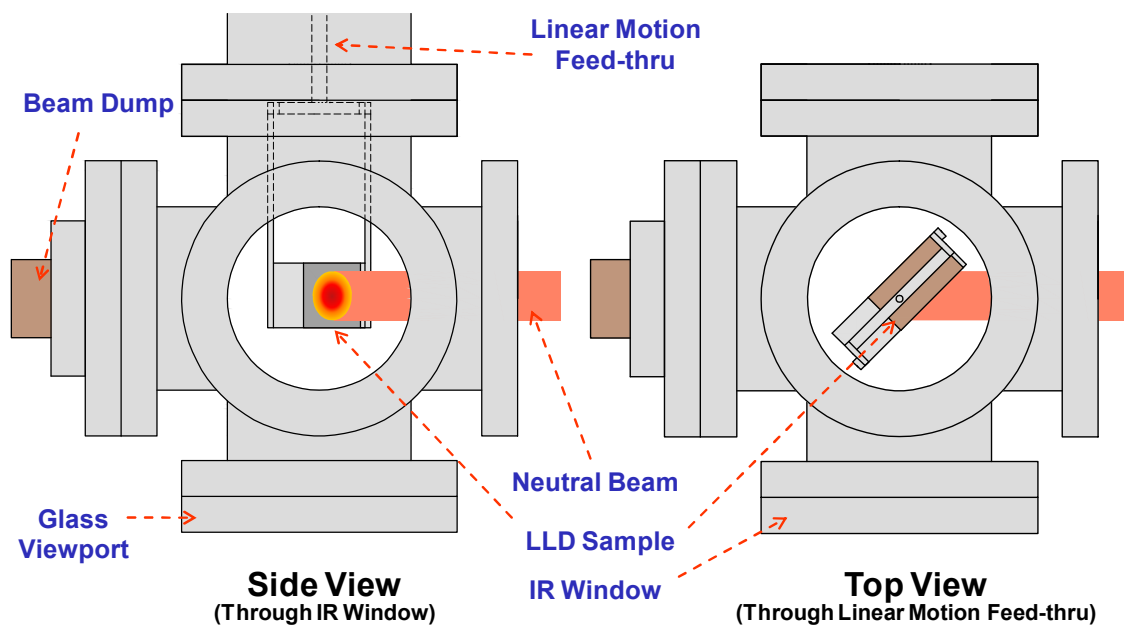


Figure 1. A view of the experimental apparatus through (a) the IR window mounted on one side of the six-way cross and (b) the linear motion feed-through mounted on top of the cross.

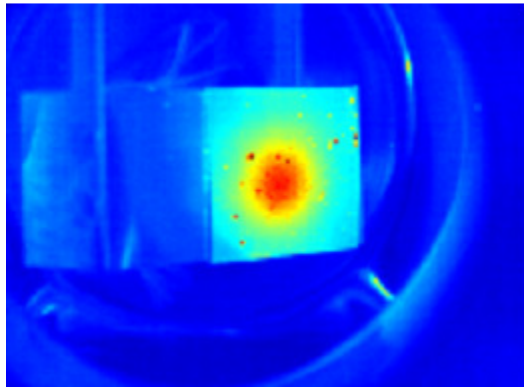


Figure 2. A false color image of the “bare” LLD sample during neutral beam exposure.

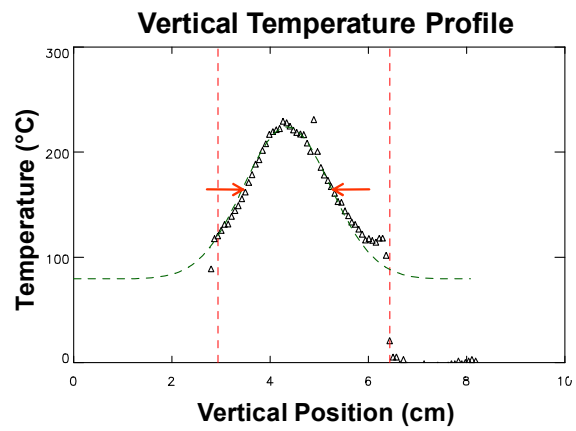


Figure 3. The vertical temperature profile on the front face of the LLD sample.

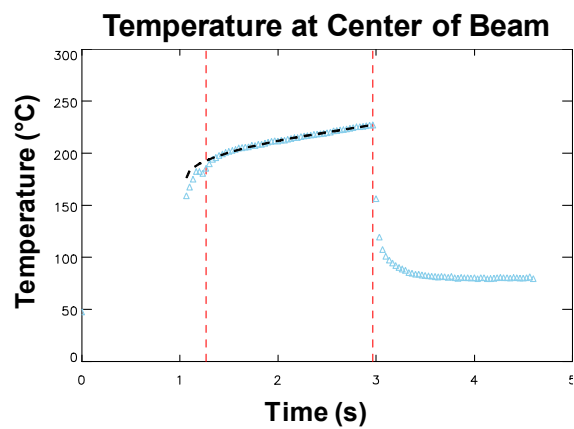


Figure 4. Thermal evolution of the front face of the bare LLD sample at the center of the beam during a  $\sim 1.8$  s exposure.



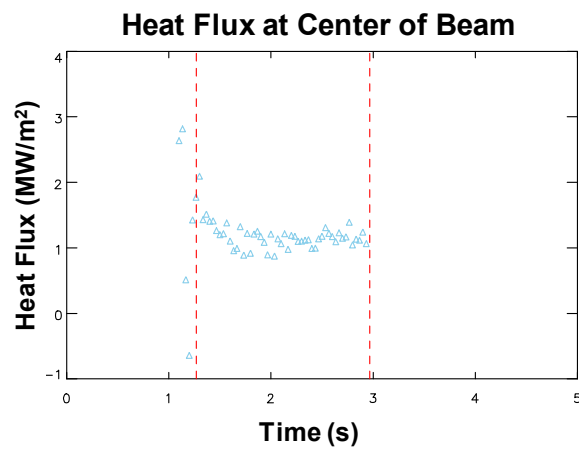


Figure 5. Heat flux at the center of the beam as determined from a 1-D numerical model.

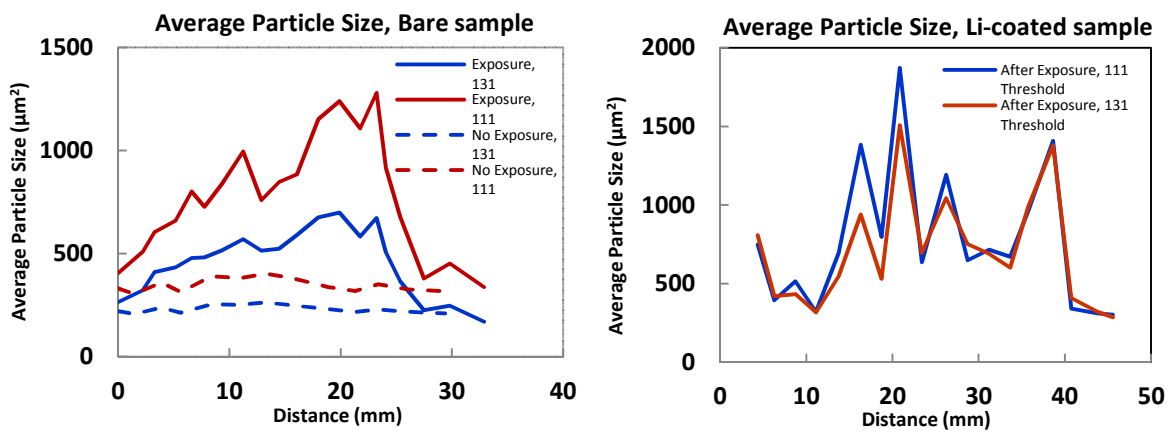


Figure 6. Average particle size plotted against distance across the surface of the bare sample (left) and Li-coated sample (right).



The Princeton Plasma Physics Laboratory is operated  
by Princeton University under contract  
with the U.S. Department of Energy.

Information Services  
Princeton Plasma Physics Laboratory  
P.O. Box 451  
Princeton, NJ 08543

Phone: 609-243-2245  
Fax: 609-243-2751  
e-mail: [pppl\\_info@pppl.gov](mailto:pppl_info@pppl.gov)  
Internet Address: <http://www.pppl.gov>